Revisiting PS191 limits on sterile neutrinos

Krasnov I. V.

INR RAS

11.04.2022

co-authors:
Dmitry Gorbunov (INR RAS, MIPT), Sergey Suvorov (INR RAS, MIPT, LPNHE UPMC)

International Conference on Quantum Field Theory, High-Energy Physics, and Cosmology, JINR, Dubna

Table of contents

Sterile neutrinos (HNL)

$$\mathscr{L} = i\bar{N}_I \gamma^\mu \partial_\mu N_I - \left(\frac{1}{2} M_N \bar{N}_I^c N_I + \hat{Y}_{\alpha I} \bar{L}_\alpha \tilde{H} N_I + h.c.\right), \quad (1)$$

- Renormalizable theory
- Experimental confirmation prospects
- SM neutrino mass scale explanation
- (Optional) Baryon asymmetry mechanism
- (Optional) Dark matter candidate

Why revisit PS191?

	PS191	T2K
Beam energy	19 GeV	30 GeV
N_{POT}	0.56×10^{19}	4×10^{21}
Detector size	$6 \times 3 \times 12\,\mathrm{m}^3$	$1.92 \times 0.56 \times 1.84\,\mathrm{m}^3$

- Original PS191 works consider only Charged Currents.
- Many attempts to account for Neutral Currents, redrawing original PS191 lines.
- 2109.03831 compares PS191 to T2K and questions the validity of revisions.
- PS191 results are overrated?

PS191

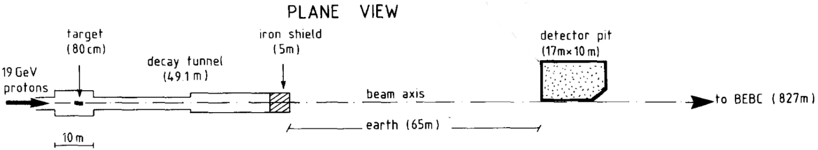

Figure 1: The layout of the PS191 experiment at CERN.

General idea:

$$N_N = N_{POT} \times \sum_H \frac{N_H}{N_{sim}} \cdot Br(H \to N\ldots) \cdot \xi_H \cdot P\,. \qquad (2)$$

No signal found, ideally no background: $N_N = 2.3$ (90% CL) according to the Poisson statistics.

HNL production

$$\mathrm{Br}(K^{\pm} \to l^{\pm} N) = |U_l|^2 \frac{\tau_K}{8\pi} G_F^2 f_K^2 M_K M_N^2 |V_{us}|^2$$
$$\times \left(1 - \frac{M_N^2}{M_K^2} + 2\frac{M_l^2}{M_K^2} + \frac{M_l^2}{M_N^2}\left(1 - \frac{M_l^2}{M_K^2}\right)\right) \times \sqrt{\left(1 + \frac{M_N^2}{M_K^2} - \frac{M_l^2}{M_K^2}\right)^2 - 4\frac{M_N^2}{M_K^2}}. \quad (3)$$

- Focusing mode: $N_{\mathrm{POT}}^{\mathrm{on}} = 0.56 \times 10^{19}$ – we only consider K^+.
- No magnetic field: $N_{\mathrm{POT}}^{\mathrm{off}} = 0.30 \times 10^{19}$, both K^+ and K^- are considered.

Geometrical Factor

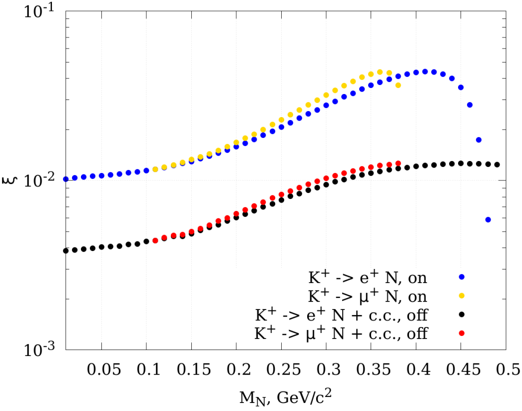

Figure 2: The geometrical factor ξ for the HNLs as a function of its mass for HNLs produced in charged kaon decays. "On"-mode stands for our simulation of working focusing system. This is the fraction of all HNL which trajectories pass through the PS191 detector.

HNL decay

$$P \approx \frac{\Delta l}{\tau_N} \frac{M_N}{p_{N_L}} = \Delta l \frac{M_N}{p_{N_L}} \sum \Gamma(N \to \ldots)$$

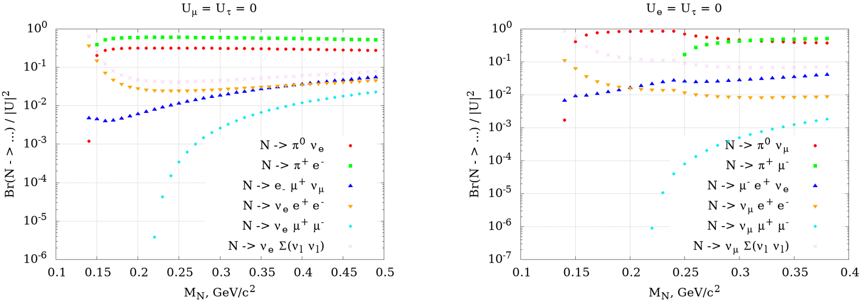

Figure 3: Sterile neutrino decay modes in case of pure electronic (left panel) and pure muonic (right panel) mixing. In this case the branching ratios do not depend on the mixing parameter $|U_\alpha|^2$.

Mixing with electron

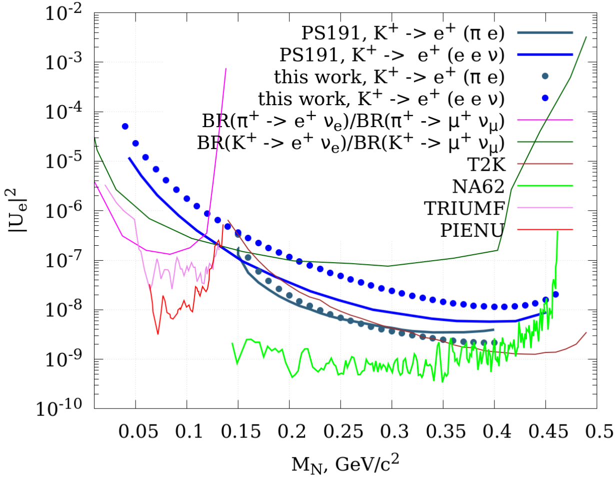

Figure 4: Limits on sterile neutrino mixing with electron neutrino.

Mixing with muon

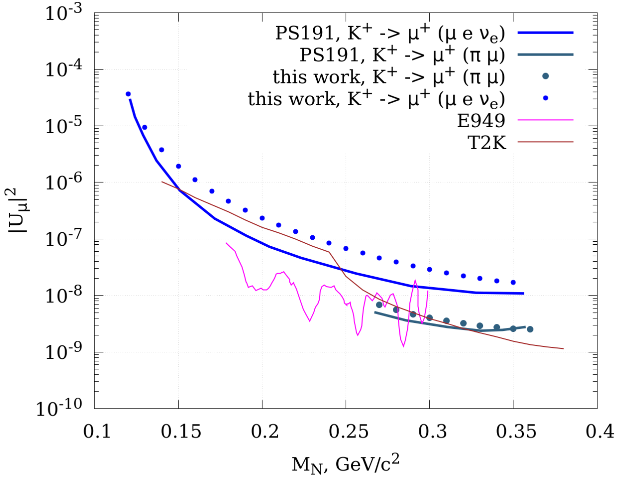

Figure 5: Limits on sterile neutrino mixing with muon neutrino.

Combined mixing

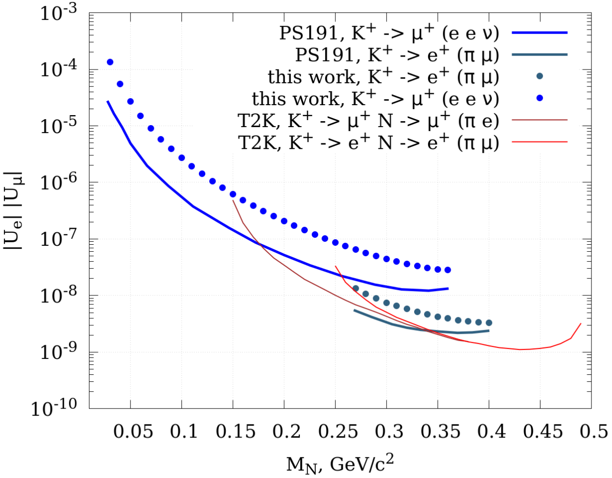

Figure 6: Limits on the product of sterile neutrino mixings with electron and muon neutrinos.

Conclusions

- We simulated the HNL production and decay within the setup of the PS191 experiment and find that their published limits are most probably too optimistic.
- It seems that the best limits they could obtain are now surpassed by later experiments, and hence there is no need to study further the PS191 performance.

Thank you for your attention!

Backup Slides

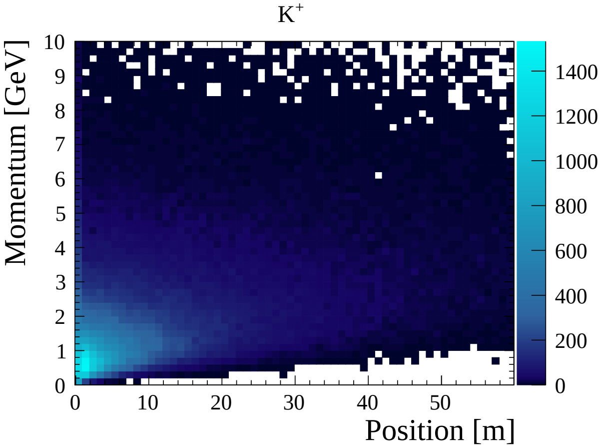

Figure 7: Distributions of 3-momentum at the decay point and travel distance of the positively charged kaons as we adopted for the "on"-mode.

Backup Slides

	in target and decay tunnel	in the beam dump	in soil outside decay tunnel
K^+ produced	83833	117493	133535
K^- produced	37439	899	6984
K_L^0 produced	19646	1824	11186
K^+ decayed in flight	92048	4572	18268
K^+ decayed stopped	446	113028	106499
K^- decayed in flight	40580	886	3856
K_L^0 decayed (in flight)	25606	1571	5479

Table 1: Decayed kaon budget for a total simulated statistics of $N_{POT} = 2 \times 10^6$.

Backup Slides

$$\Gamma\left(N\to\pi^+\mu^-\right)=\frac{|U_\mu|^2}{16\pi}G_F^2|V_{ud}|^2f_\pi^2M_N^3\cdot\left(\left(1-\frac{M_\mu^2}{M_N^2}\right)^2-\frac{M_\pi^2}{M_N^2}\left(1+\frac{M_\mu^2}{M_N^2}\right)\right)$$

$$\times\sqrt{\left(1-\frac{\left(M_\pi-M_\mu\right)^2}{M_N^2}\right)\left(1-\frac{\left(M_\pi+M_\mu\right)^2}{M_N^2}\right)},\qquad(4)$$

$$\Gamma\left(N\to\pi^+e^-\right)=\frac{|U_e|^2}{16\pi}G_F^2|V_{ud}|^2f_\pi^2M_N^3\cdot\left(1-\frac{M_\pi^2}{M_N^2}\right)^2,\qquad(5)$$

Backup Slides

$$\Gamma\left(N \to \nu_e e^+ e^-\right) = \frac{G_F^2 M_N^5}{192\pi^3} \cdot |U_e|^2 \cdot \frac{1}{4}\left(1 + 4\sin^2\theta_w + 8\sin^4\theta_w\right)\,, \tag{6}$$

$$\Gamma\left(N \to \nu_\mu e^+ e^-\right) = \frac{G_F^2 M_N^5}{192\pi^3} \cdot |U_\mu|^2 \cdot \frac{1}{4}\left(1 - 4\sin^2\theta_w + 8\sin^4\theta_w\right)\,, \tag{7}$$

$$\Gamma\left(N \to e^- \mu^+ \nu_\mu\right) = \frac{G_F^2 M_N^5}{192\pi^3} \cdot |U_e|^2 \left(1 - 8\frac{M_\mu^2}{M_N^2} + 8\frac{M_\mu^6}{M_N^6} - \frac{M_\mu^8}{M_N^8} - 12\frac{M_\mu^4}{M_N^4}\log\frac{M_\mu^2}{M_N^2}\right), \tag{8}$$

$$\Gamma\left(N \to \mu^- e^+ \nu_e\right) = \frac{G_F^2 M_N^5}{192\pi^3} \cdot |U_\mu|^2 \left(1 - 8\frac{M_\mu^2}{M_N^2} + 8\frac{M_\mu^6}{M_N^6} - \frac{M_\mu^8}{M_N^8} - 12\frac{M_\mu^4}{M_N^4}\log\frac{M_\mu^2}{M_N^2}\right) \tag{9}$$